



# Obtaining Multiple Colors and Luster after One-Time Printing with Plasma Treated PET-TiO<sub>2</sub> Fabrics

Tarig T. A. Owad<sup>1</sup> · Amel E. A. Elabid<sup>2</sup> · Renad E. M. Salih<sup>1</sup> · Syed Rashedul Islam<sup>3</sup> · Bilal Zaarour<sup>4</sup> · Yu Zhang<sup>1</sup> · Yu Xu<sup>1,5,7</sup> · Jie Min<sup>6</sup> · Jing Zhang<sup>1,5,7</sup>

Received: 1 February 2023 / Accepted: 4 June 2023 / Published online: 11 July 2023  
© The Author(s), under exclusive licence to Springer Science+Business Media, LLC, part of Springer Nature 2023

## Abstract

In this study, multiple colors and deluster polyethylene terephthalate (PET) fabrics at one-time printing were obtained by different plasma treating times. Radio frequency (13.56 MHz) plasma was employed to selectively etch on deluster polyethylene terephthalate-titanium dioxide (PET-TiO<sub>2</sub>) fabrics, which improved the surface roughness and introduced active groups. TiO<sub>2</sub> nanoparticles were exposed on the surface of the PET fabrics. The treated PET fabrics exhibited superhydrophilicity, as evidenced by the reduction of the water contact angle to zero degree (0°). A magnetic screen-printing machine was utilized to apply a paste printing consisting of blue pigment, binder, and synthetic thickener. After plasma selective etching, the delusted PET fabric with exposed TiO<sub>2</sub> improved the printability. Moreover, this work provided a simple and eco-friendly method for different surface, physical, and chemical properties of the PET fabrics. The method also enhanced the color strength rate, washing, and rubbing fastness of the PET fabrics. Thus, the printing of organic component PET fabrics could be one step toward improving print qualities after plasma etching treatment.

**Keywords** Plasma selective etching · Delustered PET · TiO<sub>2</sub> nanoparticles · Printability · Color fastness

## Introduction

Textile fabrics are used for a wide variety of functions and applications [1]. As textile substrates, PET printing materials are the second-most popular kind [2]. PET fiber has a huge market share of over 80% and is the most popular, economical, and versatile synthetic material worldwide due to its excellent wide range of mechanical, chemical, and thermal properties [3, 4]. Moreover, it has played an essential role in daily use. The textile garment industry uses it due to its flexibility, durability, high mechanical strength, low cost with high chemical resistance, highly hydrophobic, easy recycling, and so on [5]. However, the PET fabric's molecular structure has lack of polar groups (-OH, -COOH, -NH<sub>2</sub>, etc.) on its polymer backbone, which have led to bad wear experience. Additionally, it is unable to interact with cationic or anionic dyes [6]. Unfortunately,

it is challenging to get fully shaded color, due to its intrinsically great refractive index ( $n = 1.725$ ), which reflects a significant amount of light from the surface [7].

Due to poor adhesion and high hydrophobicity with a high water contact angle, i.e., dyeing, printing, and finishing are more challenging and complicated [8–10]. These deficiencies in the functional characteristics of PET fabrics have limited their further use [11, 12]. Hossain, M.A. et al. have investigated the surface characteristics modification technique. The treatment of PET fibers for screen-printing is critical, and it represents an important role in printing media; for example, low surface energy and low surface roughness lead to effects on the adhesion of coating materials. Due to the surface characteristics, PET fabrics are not consistent enough for printing, and thus, indicating low color yield in grand easy bleeding. Moreover, before printing, the surface characteristics of PET fabric have not been changed significantly, as a result, the color strength and color fastness qualities of printed fabric are reduced [13]. Abou Elmaaty, T. et al. have studied one-step thermochromic pigment printing of 100% cotton and 50/50% (cotton/polyester) blend. The results have indicated that the color fastness to washing and rubbing is excellent, the surface roughness is lower, the pigment particles are unable to disperse through fibers, and residual remained on the surface of the fibers. On the other hand, the paste printing absorption is significantly less on PET fabric, resulting in less K/S value (representing absorption) of printed fabric [14]. Besides, there are still concerns about obtaining durable printing quality, especially, about color fastness to washing, crocking, and light that cause colors to transfer to another cloth. To increase legal and environmental requirements for the chemical printing process, it is better to use light chemicals and low power exhaustion [15]. Moreover, it is needed to modify the fabric to reduce pollution, minimize damage, and improve the absorption quality of printing on the fabric [16–18].

Pransilp et al., have used plasma nano-modification of PET fabrics for pigment adhesion to functionalize the printed fabrics with durable printing quality and desired printing layer thickness, and the fabric surface characteristics and roughness have to exist to the used pigment paste material. Undoubtedly, there are several conventional techniques to fabricate printable characteristics surfaces like dip-coating, chemical padding, and so on. Typically, they require hazardous chemical compounds and produce vast amounts of wastewater which are considered environmentally harmful [19–21]. Compared with traditional techniques, plasma technology has many advantages of increasing surface functionality and cost-saving since it does not need to use of water or chemicals [22–24].

Plasma-etching treatment creates etching on fiber surfaces and increases active surface area on fibers [25]. It also helps to change the surface structure of fabric without impacting the bulk of the material [26]. In order to prevent any substantial harm from ion bombardment, neutral atom rich plasmas with relatively moderate ion densities are preferred for the treatment of sensitive and heat-sensitive polymer materials. Potential energy interactions with the surface have a greater impact on neutral radical interactions with surfaces than kinetic energy interactions do. The entering plasma particle must have sufficient energy to pass the activation energy barrier for chemical reactions to interact with an exposed surface. This can be managed by altering the discharge's feed gas flow rate, gas composition, plasma power, and operating pressure, among other parameters. In addition, surface roughness affects the coating adhesion and can be increased by plasma etching [27].

Elabid et al. have modified the surface of PET fabric using the atmospheric pressure with  $O_2/Ar$  plasma treatment method to tailor the surface morphology, chemical structure, and enhance low-temperature dyeability through dispersing dyes. Interestingly, incorporating inorganic nanoparticles such as  $TiO_2$  into the PET fabric matrix provides them with

some novel and unique properties [28]. Namely,  $\text{TiO}_2$  nanoparticles have been used to improve the hydrophilicity properties of PET fabric [29].

In our previous study, it was observed that the selective etching of PET fibers (organic) by plasma treatment led to the exposure of  $\text{TiO}_2$  particles (inorganic) on the fabric surface due to the disparity in etch rate between organic and inorganic components [4]. That process resulted in the development of a rough, hydrophilic and durable surface of polyethylene terephthalate (PET) fabric, which was believed to enhance its printing performance. In the current study, a higher power supply and gas flow are employed to create a rough and hydrophilic surface, and the printing characteristics of PET with different plasma treatment times are investigated. By varying the treatment time, it is possible to achieve multiple colors in a single printing with plasma selective etching. Moreover, the paste printing with PET- $\text{TiO}_2$  fabric surface has been extensively enhanced and provides better K/S values in printing.

## Experimental

### Materials

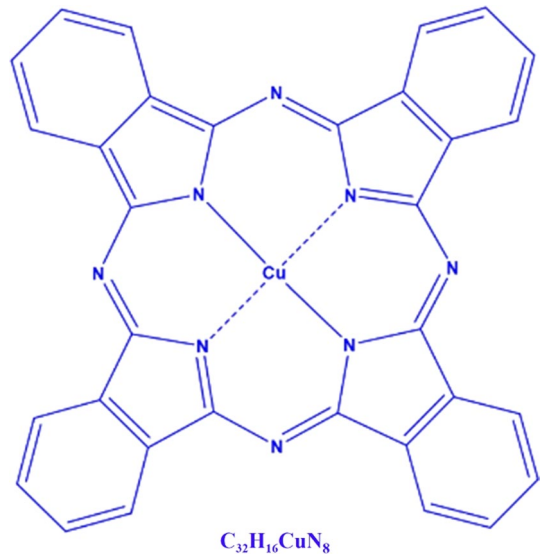
Argon and oxygen (99.99%) in plasma etching were supplied by Shanghai Cheng Gong Gas Industry Co. Ltd., China. Phthalocyanines ( $\text{C}_{32}\text{H}_{16}\text{CuN}_8$ ) were purchased from Shanghai Silian pigment Co. Ltd., China. The plain weave pure PET fabric (weight of  $\sim 50 \text{ g m}^{-2}$ ), as well as two types of delustered PET fabrics with different percentages of  $\text{TiO}_2$  nanoparticles, i.e., PET- $\text{TiO}_2\text{-S}_L$  ( $< 0.5 \text{ wt\%}$ , weight  $\sim 72.41 \text{ g m}^{-2}$ ) and PET- $\text{TiO}_2\text{-S}_H$  ( $< 2.0 \text{ wt\%}$ , weight  $\sim 64.7 \text{ g m}^{-2}$ ) were provided from Hua Fang Co. Ltd., China. Pigment Blue 15 was delivered from Zhejiang Longsheng Group Co. Ltd., China (Lonsen). Polyacrylic acid (Synthetic Thickening Agent) was purchased from Xianhua (Shanghai) Bio-Chemical Co. Ltd., China. Polyacrylate emulsion (binder agent) was purchased from Zhejiang Transfer Co. Ltd., China. The water utilized in experiments was deionized and distilled. Standard detergents were purchased from Shanghai White Cat Special Chemical Company and Shanghai Technical Supervision of Textile Industry, China. The chemical structure of phthalocyanine was shown in Fig. 1.

The fabric samples were washed in distilled water in an ultrasonic cleaner for 120 min at  $60 \text{ }^\circ\text{C}$  to minimize contamination, then taken out and dried in an oven at  $70 \text{ }^\circ\text{C}$  for 1 h. The cleaned fabrics were cut into  $25 \times 25 \text{ cm}$  dimensions for the experiment. The fabric samples were ironed to achieve a flat surface. It was essential to keep the PET fabrics stable in a screen-printing machine to print the fabric samples.

### Plasma Treatment Process

The plasma etching treatment was described in detail in our previous work [4]. In order to transfer the design of DHU logo to the fabrics, the paperboard was used. The reactor was filled with oxygen (100 sccm), argon (10 sccm), and the working pressure was maintained at 300 mTorr. Deserved to be mentioned, etch rates typically increase with oxygen atom concentration in the plasma [30, 31]. The highest etch rates involved pure oxygen followed by air, nitrogen, and argon gases [32]. While, Ar plasma provide a more efficient energy transfer due to the heavy ions incident on the sample surface. Ar ions allow ion-induced

**Fig. 1** The structure of C.I. Pigment Blue 15 used in this work



chemical etching processes that can contribute to synergistic effects when  $O_2$  is added [33]. The fabrics were treated at 400W power with different times (1, 4, and 7 min).

### Screen-Printing Process

Briefly, the pigment paste was prepared by 15 g of polyacrylate emulsion, 0.2 g of polyacrylic acid sodium salt, and 2.5 g of blue pigment dyeing solutions, and these were added into demineralized water of 32.3 g for a total recipe of 50 g. After that, an electric mixer was used to stir the mixture evenly and carefully until the heavy pigment paste phase was formed. In order to solidify the pigment paste, the paste printing was mixed by an electric mixer for 20 min under atmospheric pressure at room temperature. The paste printing was slurry, well homogenized, and applied to the fabric samples using a screen-printing of 70 mesh, a squeegee diameter of 12 mm. The screen-printing frame was made of nylon wire with a mesh density of 300 fibers per centimeter. The pigment printing process was achieved using a magnetic screen printing machine from (Zimmer, Austria) with a printing speed of about 32.3 mm/s. The pigment paste was sneaked through the screen mesh and carried to the fabric under a magnetic stick of  $\varnothing$  63.6 mm. The pigmented fabrics were dried at 80 °C for 5 min and cured at 150 °C for 3 min in a temperature-controlled oven, as shown in Fig. 2. All the experiments were carried out using distilled water. The pigmented samples were assessed according to the standard test methods to decide whether the plasma treated fabrics were similar or improved, showing properties compared to untreated fabrics.

### Fabric Characterizations

The surface morphology of samples was observed by using field emission scanning electron microscopy (FE-SEM, S-4800 Hitachi, Japan) and fitted with energy dispersive spectrometer (EDS). Surface morphologies of the samples before and after the plasma etching treatment were studied using atomic force microscopy (AFM, Agilent

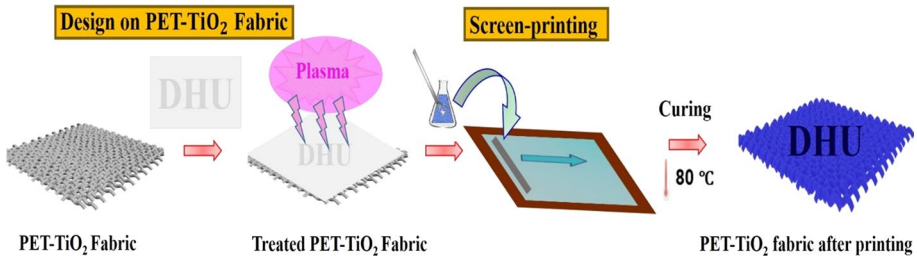


**Fig. 2** The schematic diagram of designing the pattern with plasma selective etching system and screen printing process on fabric surface

5500). The changes in the surface chemical composition of the fabrics were analyzed by X-ray photoelectron spectroscopy (XPS) measurements with a Kratos Axis Ultra DLD XPS (Thermo Fisher ESCALAB 250Xi, USA) using an Al K<sub>α</sub> X-rays radiation source (1253.6 eV). For XPS spectra processing, advantage software was employed to deconvolve and analyze the C1s, O1s, and Ti2p peaks.

To investigate the connection of pigment adhesion to the wettability behavior of the samples, static water contact angles (WCAs) on the sample’s surfaces were measured by a DropMeter™ professional A-200 computer-video-processed goniometry (Haishu Maishi Testing Technology Co. Ltd., Ningbo, China) and sliding angle (S. A.). Distilled water (5 μl) was dropped on the surface of the fabrics and the water contact angles were read immediately.

The reflectance measurements of printing fabrics were measured using a Datacolor SP600 + Spectrophotometer (Datacolor Co. Lawrenceville, NJ, USA), and the measurement wavelength range was from 360 to 700 nm. The color strength (K/S value) of the printed samples was calculated by the Kubelka–Munk Eq. (1).

$$K/S = (1 - R)^2 / 2R \tag{1}$$

where K/S is the ratio of absorption and scattering coefficient, and the reflectance (R) is determined at the wavelength from the highest absorbance of the used pigment color on printed fabric.

Measurement results were selected at the λ<sub>max</sub>. The color strength rate (I) was determined by Eq. (2).

$$I = \left\{ (K/S)_A - (K/S)_B / (K/S)_B \right\} \times 100\% \tag{2}$$

where (K/S)<sub>A</sub> and (K/S)<sub>B</sub> are the color yield of the treated and untreated printed samples.

The color washing fastness was achieved in the SW-12A Tester (Wenzhou Darong Textile Instrument Co. Ltd., China) and according to the soaping test (ISO 105-C10:2006) standard. The changing in the color of the printed fabrics (according to ISO105-A02:1993) and the staining (according to ISO 105-A03:1993) of the adjacent multifiber fabric (Multifiber D.W., adjacent fabric, BS ISO 105-F10:1989) were evaluated using grey scales under the D65 standard light source. The rubbing fastness of the printed fabrics was evaluated with the Y571L rubbing and scrubbing color fastness tester, and the samples were rated according to ISO 105-X12-2001. The samples’ names and conditions used in the current study were listed in Table 1.

**Table 1** The sample names and conditions used in the experiment

Treatment method	Plasma etching			
	0 min	1 min	4 min	7 min
Samples name	PET	PET-1	PET-4	PET-7
	PET-TiO <sub>2</sub> -S <sub>L</sub>	PET-TiO <sub>2</sub> -S <sub>L</sub> -1	PET-TiO <sub>2</sub> -S <sub>L</sub> -4	PET-TiO <sub>2</sub> -S <sub>L</sub> -7
	PET-TiO <sub>2</sub> -S <sub>H</sub>	PET-TiO <sub>2</sub> -S <sub>H</sub> -1	PET-TiO <sub>2</sub> -S <sub>H</sub> -4	PET-TiO <sub>2</sub> -S <sub>H</sub> -7

S<sub>L</sub> with TiO<sub>2</sub> < 0.5 wt%, S<sub>H</sub> with TiO<sub>2</sub> < 2.0 wt% in the fabric

## Results and Discussion

### Surface Morphology Analysis of the Samples

Figure 3a shows that the surface of the control PET fabric sample was smooth and free from roughness and particles. However, the surface of PET-7 fabric became rough with connected forming lines of humps and ridges because of Ar/O<sub>2</sub> plasma-etching, as shown in Fig. 3b. The physical and chemical etching effects of active particles like ions and radicals in the Ar/O<sub>2</sub> plasma etching onto the surface of the fabrics were responsible for these results [34]. The control PET-TiO<sub>2</sub>-S<sub>L</sub> fabric had a smooth surface with fine nanoparticles, as shown in Fig. 3c. Meanwhile, a control PET-TiO<sub>2</sub>-S<sub>H</sub> fabric surface was rough with a few sparsely distributed nanoparticles, as shown in Fig. 3e. After 7 min plasma etching, the PET-TiO<sub>2</sub>-S<sub>L</sub>-7 fabric sample surface became rougher with deeply etching irregular pits, humps, and nanoparticles, as shown in Fig. 3d. Nevertheless, these irregular pits, nanoparticles, and humps were a larger size than those observed in the PET-TiO<sub>2</sub>-S<sub>H</sub>-7 fabric sample surface, as shown in Fig. 3f, which could be attributed to the TiO<sub>2</sub> nanoparticles protruding from the inner of the fiber to its outer surface.

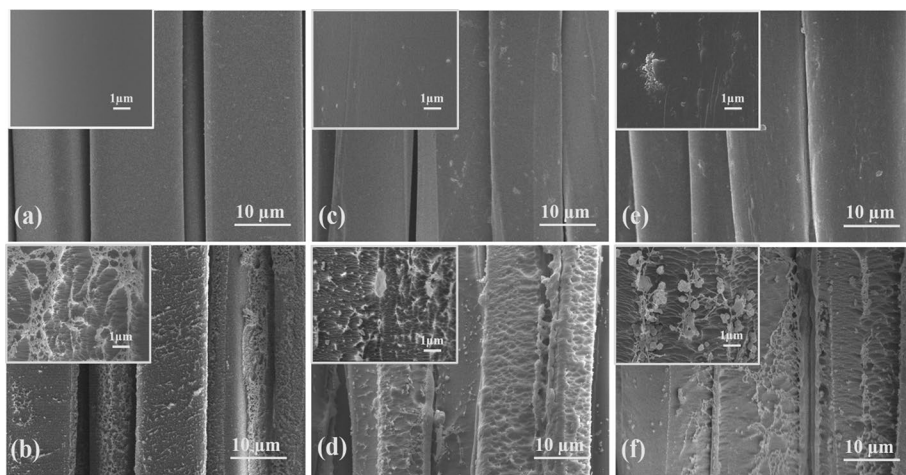


**Fig. 3** The FE-SEM images of PET (a), PET-7 (b), PET-TiO<sub>2</sub>-S<sub>L</sub> (c), PET-TiO<sub>2</sub>-S<sub>L</sub>-7 (d), PET-TiO<sub>2</sub>-S<sub>H</sub> (e), and PET-TiO<sub>2</sub>-S<sub>H</sub>-7 (f); insets are their corresponding high magnified images

The EDS spectra of the surface structures were measured and the relative surface atomic percentage of Ti, C, and O of samples are presented in Fig. 4. The EDS spectra of the untreated and treated PET fabrics are shown in Fig. 4a–d, where O and C elements were observed, however, Ti was not appeared. The Ti in the surface of PET-TiO<sub>2</sub>-S<sub>L</sub>-7 fabric with a content of 2.88% was confirmed by EDS spectra in Fig. 4e. Interestingly, the Ti element increased from 0.31% to 10.30% on PET-TiO<sub>2</sub>-S<sub>H</sub>-7 fabric surface, as shown in Fig. 4c–f. Ti element derived from TiO<sub>2</sub> nanoparticles in PET-TiO<sub>2</sub>-S<sub>L</sub>-7 and PET-TiO<sub>2</sub>-S<sub>H</sub>-7 fabrics after the etching and bombardment processes of active plasma particles and the removal out of the organic PET thin layer was covered by TiO<sub>2</sub> nanoparticles [35]. More Ti element atomic percentage indicated that more TiO<sub>2</sub> nanoparticles were exposed after plasma treatment as verified later through XPS. The platinum (Pt) element was produced by metallic sputtering for FE-SEM measurement.

### Surface Topography (AFM Analysis)

AFM images of topographic modifications and surface roughness of the samples before and after plasma etching is shown in Fig. 5. As shown in Fig. 5a, the untreated PET pure surface showed a fairly smooth texture and flat surface with a roughness value of 14.74 nm. In contrast, Fig. 5d presented the rougher surface with a small pit-like structure having a surface roughness of 28.6 nm for 7 min treatment. While the dull untreated PET-TiO<sub>2</sub>-S<sub>L</sub> fabric in Fig. 5b displays a relatively smooth surface with a few rides to the craters having a surface roughness of 14.38 nm. In contrast, Fig. 5e exhibits a progressive change in surface roughness with nano-sized particle protuberances having a surface roughness of 31.25 nm. Figure 5c shows untreated dull PET-TiO<sub>2</sub>-S<sub>H</sub> with small hills displaying a few rides to the pits, which directed surface roughness of 26.59 nm. However, following the plasma treatment for 7 min, in Fig. 5f, the surface of the fabrics

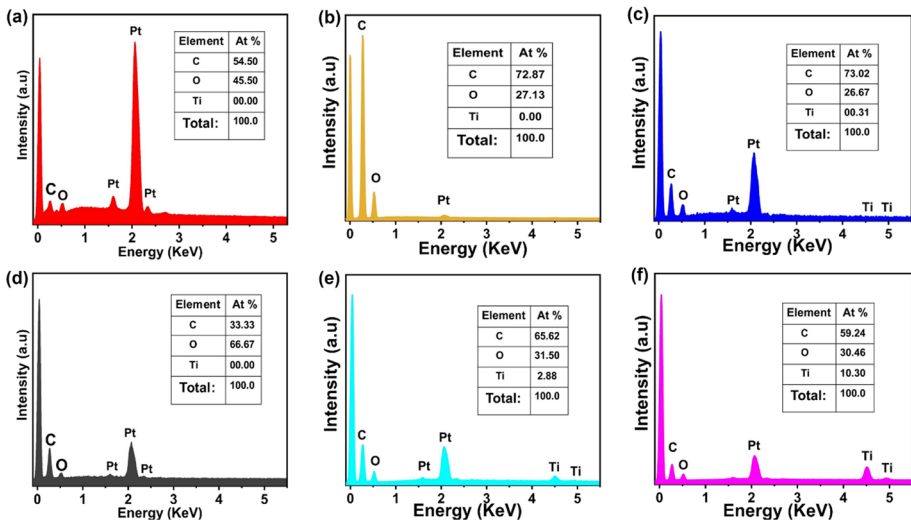


**Fig. 4** The EDS test of PET (a), PET-TiO<sub>2</sub>-S<sub>L</sub> (b), PET-TiO<sub>2</sub>-S<sub>H</sub> (c), PET-7 (d), PET-TiO<sub>2</sub>-S<sub>L</sub>-7 (e), and PET-TiO<sub>2</sub>-S<sub>H</sub>-7 (f)

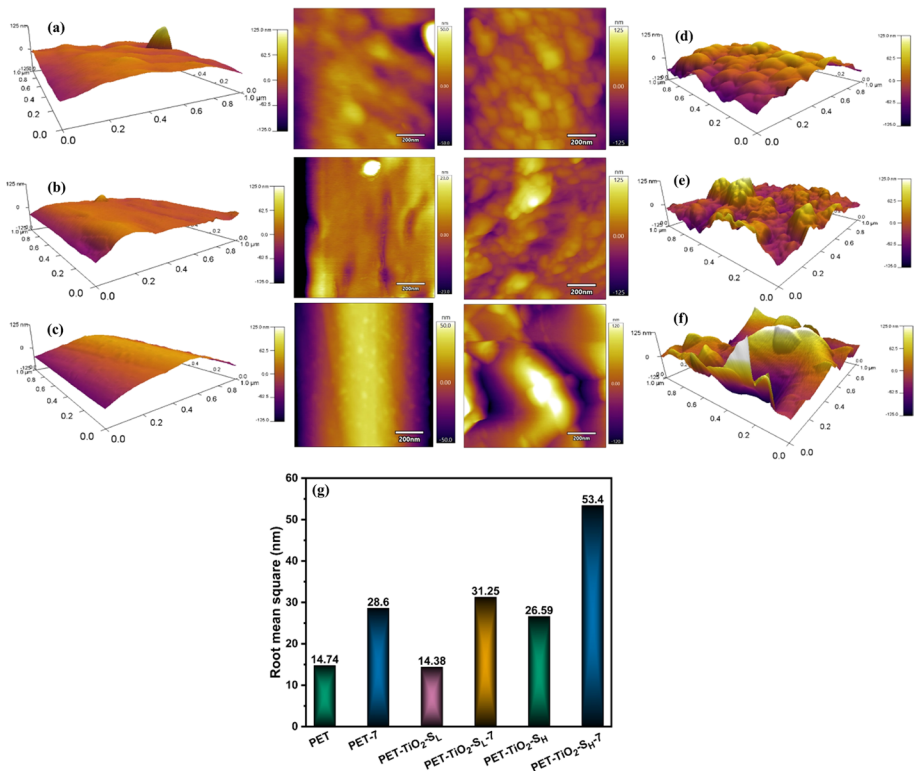


**Fig. 5** Two- and three-dimensional AFM images of PET fabric (a), PET-TiO<sub>2</sub>-S<sub>L</sub> fabric (b), PET-TiO<sub>2</sub>-S<sub>H</sub> fabric (c), PET-7 fabric (d), PET-TiO<sub>2</sub>-S<sub>L</sub>-7 fabric (e), PET-TiO<sub>2</sub>-S<sub>H</sub>-7 fabric (f), and the roughness value (RMS) (g)

provided a broad and rough wavy after the exposition of the TiO<sub>2</sub> nanoparticles on a dull PET-TiO<sub>2</sub>-S<sub>H</sub> surface and the edges of the hill, thus, relatively increased the surface roughness to 53.4 nm.

The R. F. plasma generated an increase in surface roughness by removing organic components from the PET-TiO<sub>2</sub> samples; meanwhile, it introduced polar groups onto the surface. At the same time, conspicuous TiO<sub>2</sub> nanoparticles were exposed on the PET fiber surface, significantly increasing surface roughness morphology [36]. In general, a rough surface provides more capacity for the fabric to capture paste and water, and also facilitate the penetration of paste inside the PET fabrics [10]. As a result, better surface energy, wettability, and printability of the treated dull PET-TiO<sub>2</sub> samples improved significantly.

### Surface Chemical Composition

The XPS analysis scan results were used to investigate the chemical composition of the fabric surface samples. The high-resolution spectra of C1s, O1s, and Ti2p are shown in Figs. 6, 7, and 8. Proportions of C1s, O1s, and Ti2p of the samples are listed in Table 2. C1s deconvolution analysis of PET, PET-TiO<sub>2</sub>-S<sub>L</sub>, and PET-TiO<sub>2</sub>-S<sub>H</sub> are also shown in Fig. 6a–d, b–e, and c–f, respectively. Deconvolution analysis of C–C/C–H (284.89 eV),



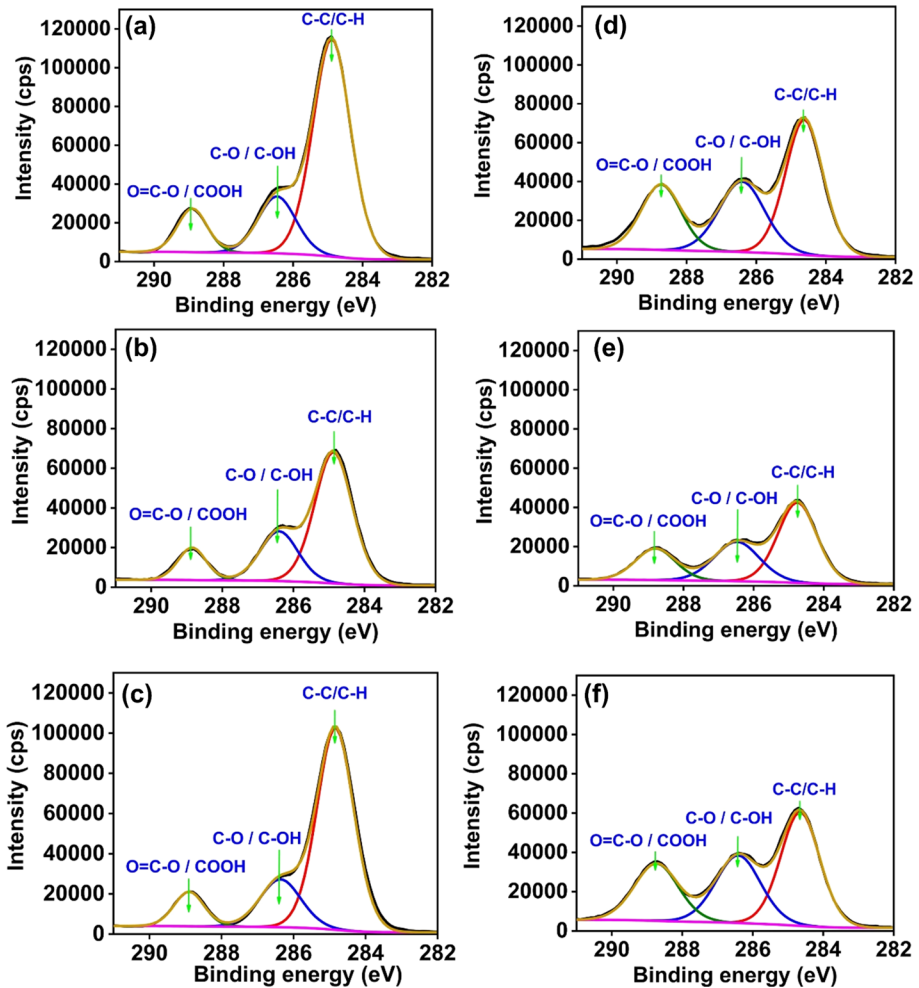


**Fig. 6** Deconvoluted XPS spectra of untreated fabrics (a) PET, (b) PET-TiO<sub>2</sub>-S<sub>L</sub>, (c) PET-TiO<sub>2</sub>-S<sub>H</sub>, and plasma-treated fabrics, (d) PET-7, (e) PET-TiO<sub>2</sub>-S<sub>L</sub>-7, (f) PET-TiO<sub>2</sub>-S<sub>H</sub>-7 fabrics for C1s, respectively

C–O/COH (286.48 eV), and O–C=O/COOH (288.9 eV) with C1s was carried out by using XPS PEAK software for PET samples. Moreover, the C1s deconvolution peaks of PET-TiO<sub>2</sub>-S<sub>L</sub> were seen at C–C/C–H (284.88 eV), C–O/COH (286.4 eV), and O–C=O/COOH (288.88 eV), respectively. Meanwhile, the C1s deconvolution peaks of PET-TiO<sub>2</sub>-S<sub>H</sub> were noticed at C–C/C–H (284.88 eV), C–O/COH (286.4 eV), and O–C=O/COOH (288.8 eV), correspondingly. After plasma treatment, the intensity of C–C/C–H bonding decreased, while the intensity of C–O and C=O functionality increased. This corresponded to the increase of O element atomic ratio in EDS and confirmed introduction of more polar oxygen groups like C–O, COH, O–C=O, and –COOH on the fabric surface after plasma treatment. The reactive plasma species assaulted the fabric’s surface, breaking C=O, C–C, and C–H bonds; oxygen atoms/radicals interacted with carbon radicals, and forming oxygen groups on the surface [34].

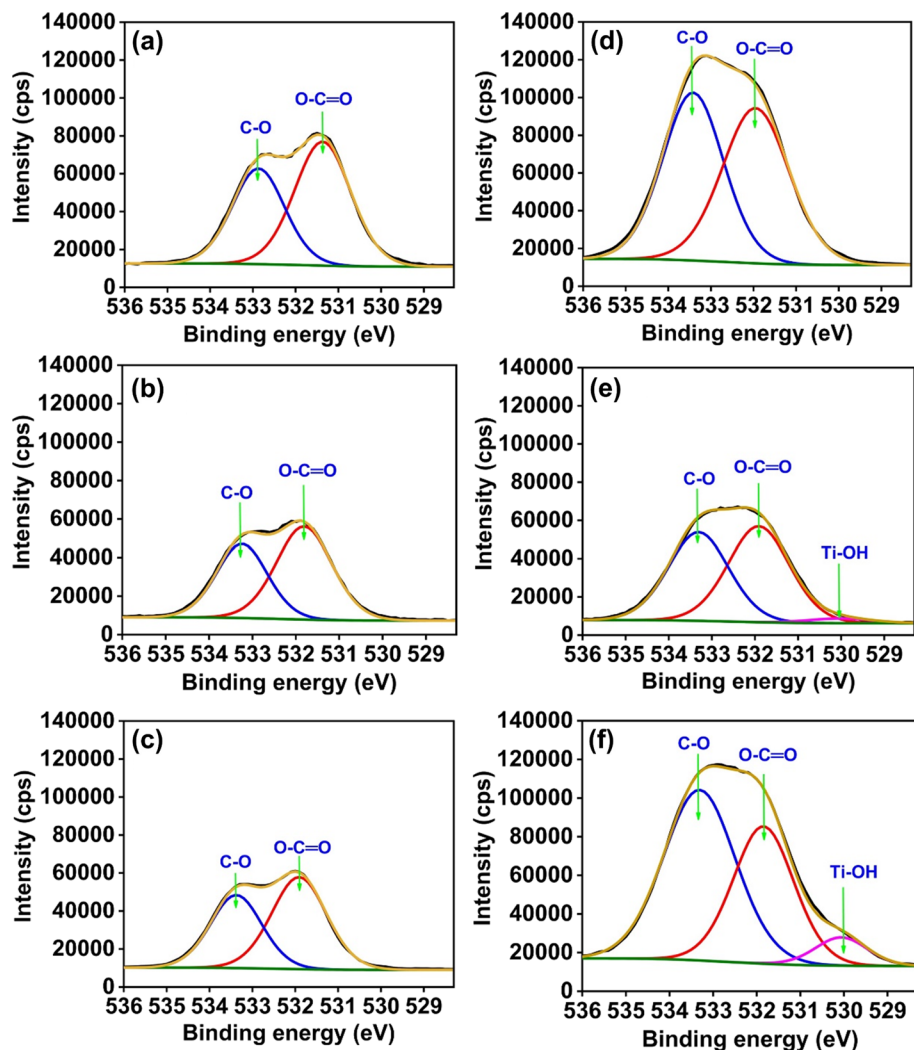


**Fig. 7** Deconvoluted XPS spectra of untreated fabrics (a) PET, (b) PET-TiO<sub>2</sub>-S<sub>L</sub>, (c) PET-TiO<sub>2</sub>-S<sub>H</sub>, and plasma-treated fabrics, (d) PET-7, (e) PET-TiO<sub>2</sub>-S<sub>L</sub>-7, (f) PET-TiO<sub>2</sub>-S<sub>H</sub>-7 fabrics for O1s, respectively

O1s deconvolution analysis of PET, PET-TiO<sub>2</sub>-S<sub>L</sub>, and PET-TiO<sub>2</sub>-S<sub>H</sub> are shown in Fig. 7a–d, b–e, and c–f, respectively. The C1s deconvolution peaks of PET were apparent at about 532.92 (C–O/COH) and 531.38 eV (O–C=O/COOH). Likewise, the O1s peaks of PET-TiO<sub>2</sub>-S<sub>L</sub> sample appeared at about 533.28 eV (C–O/COH) and 531.83 eV (O–C=O/COOH). While the O1s peaks of PET-TiO<sub>2</sub>-S<sub>H</sub> sample appeared at about 533.35 eV (C–O/COH) and 531.9 eV (O–C=O/COOH). Moreover, a new peak of O1s of PET-TiO<sub>2</sub>-S<sub>L</sub> and PET-TiO<sub>2</sub>-S<sub>H</sub> samples appeared at about 530 eV (Ti–OH) [37]. After plasma treatment of 7 min, the atomic ratio of [O]/[C] for untreated PET sample was found to be 31.40% and after treatment oxygen content increased to 61.10%. Besides, the atomic ratio of [O]/[C] for PET-TiO<sub>2</sub>-S<sub>L</sub> increased from 36.14 to 60.97%, and 27.35 to 69.25% for PET-TiO<sub>2</sub>-S<sub>H</sub>, respectively, as listed in Table 2. These significant changes

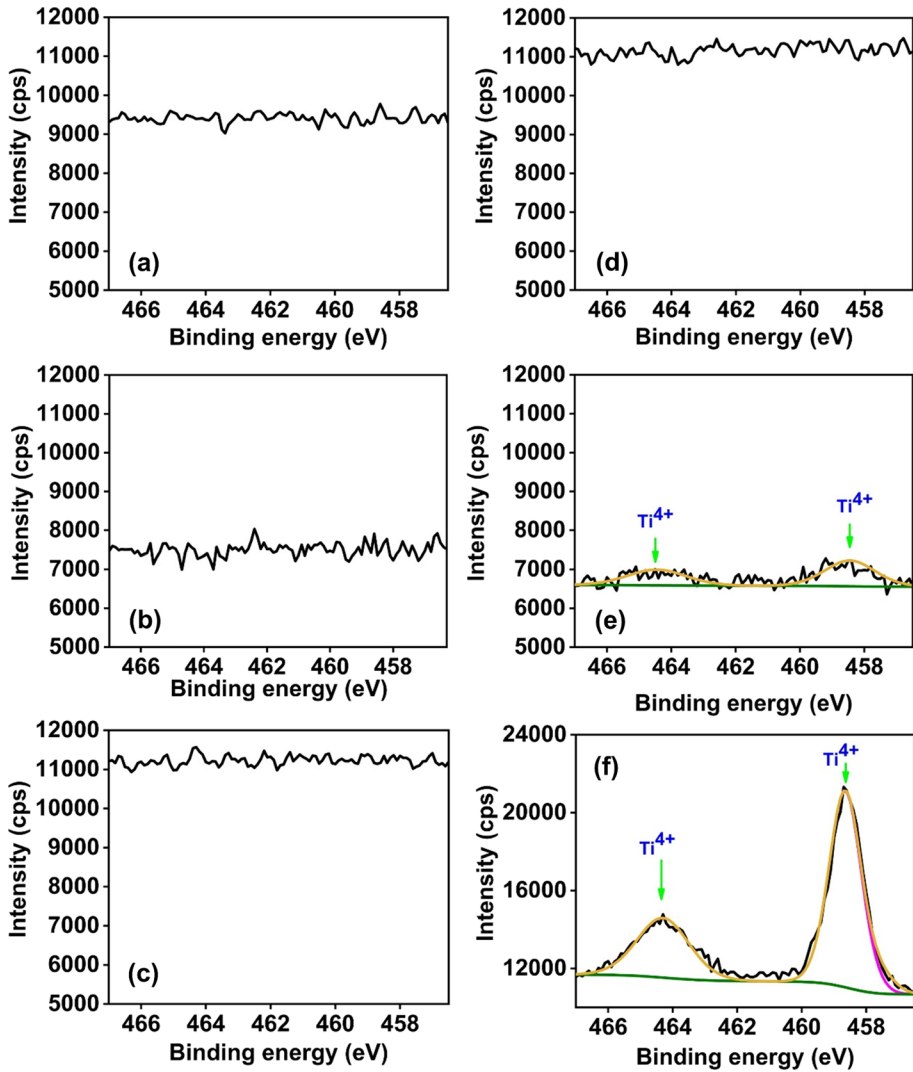


**Fig. 8** Deconvoluted XPS spectra of untreated fabrics (a) PET, (b) PET-TiO<sub>2</sub>-S<sub>L</sub>, (c) PET-TiO<sub>2</sub>-S<sub>H</sub>, and plasma-treated fabrics, (d) PET-7, (e) PET-TiO<sub>2</sub>-S<sub>L</sub>-7, (f) PET-TiO<sub>2</sub>-S<sub>H</sub>-7 fabrics for Ti<sub>2</sub>p, respectively

**Table 2** Atomic concentration of samples

Samples NAME	Atomic concentration (%)			Atomic ratio (%)	
	C1s	O1s	Ti2p	[O]/[C]	[Ti]/[C]
PET	76.1	23.9	–	31.40	–
PET-7	62.07	37.93	–	61.10	–
PET-TiO <sub>2</sub> -S <sub>L</sub>	73.45	26.55	–	36.14	–
PET-TiO <sub>2</sub> -S <sub>L</sub> -7	61.76	37.66	0.58	60.97	1.54
PET-TiO <sub>2</sub> -S <sub>H</sub>	78.52	21.48	–	27.35	–
PET-TiO <sub>2</sub> -S <sub>H</sub> -7	58.45	40.48	1.07	69.25	2.64

in fiber content revealed that the fabric had been oxidized significantly due to the Ar/O<sub>2</sub> plasma treatment [34].

The XPS spectra of Ti2p peaks are shown in Fig. 8. There is no peak related to Ti 2p spectra in pure PET samples before and after plasma etching treatment. However, for the PET-TiO<sub>2</sub>-S<sub>L</sub> fabrics, there were two small deconvoluted peaks in the Ti2p region at 458.44 (Ti<sup>4+</sup> 2p<sup>3/2</sup>) and 464.47 eV (Ti<sup>4+</sup> 2p<sup>1/2</sup>) after 7 min plasma treatment. The atomic concentration of the Ti2p element increased to 1.54%. Moreover, after 7 min plasma treatment, the PET-TiO<sub>2</sub>-S<sub>H</sub> fabric showed two deconvolution peaks in the Ti 2p region at 458.7 eV (Ti<sup>4+</sup> 2p<sup>3/2</sup>) and 464.3 eV (Ti<sup>4+</sup> 2p<sup>1/2</sup>). The atomic concentration of the Ti2p element also increased to 2.64%.

The organic component of the dull PET-TiO<sub>2</sub> fabrics shared a different etches rate to the TiO<sub>2</sub> particles, since it was easily removed, and the particles remained on the surface of the fibers [4].

### Hydrophilicity: Water Contact Angle Analysis

The water contact angle measurements before and after plasma treatment were used to investigate the effects of plasma etching on the surface of fabrics, as shown in Fig. 9. The initial water contact angle values of the three untreated samples (PET, PET-TiO<sub>2</sub>-S<sub>L</sub>, and PET-TiO<sub>2</sub>-S<sub>H</sub>) were 138.3°, 134.3°, and 123.9°, respectively. Following the plasma treatment at 1 min, the contact angle values decreases sharply from (138.3°, 134.3°, and 123.9°) to (30.3°, 20°, and 0°), respectively. With the increase of plasma treatment time at 4 min, the contact angle values of treated samples diminished rapidly to 0°. Likewise, the contact angle values of samples at 7 min plasma treated fabric declined to 0°.

### Effect of Plasma-Etching on the Coloration of Different Fabrics

Figure 10 shows the PET-TiO<sub>2</sub>-S<sub>L</sub> fabric samples after printing with different plasma treating time. The printing process was carried out using different treatment times of 1, 4, and 7 min, respectively. Compared to treated samples, the color of original sample is the lightest. Samples treated for 4 and 7 min have the darkest color. This indicates that the samples could be obtained with different colors by controlling the plasma treatment time.

As shown in Fig. 11, photos of the untreated and plasma-etched fabrics after 7 min of pigment paste application were obtained. The printed fabrics shows a significant difference in shade depth between the treated and untreated samples. Notably, the DHU design on the printed fabric samples exhibits a distinct shade depth color, which is an intriguing observation.

The surface morphologies of the printed samples were observed by FE-SEM, as shown in Fig. 12. Figure 12a shows that the surface of the printed PET-pure fabric is smooth, uniform, and homogeneous with pigment paste particles. However, the printed PET-4 fabric has a rough surface and some pigment paste particles on the surface, as shown in Fig. 12b. Figure 12c demonstrates that the surface of the printed PET-TiO<sub>2</sub>-S<sub>L</sub> fabric is rough with some particles on it. Compared to the printed PET-TiO<sub>2</sub>-S<sub>L</sub>, Fig. 12d exhibits that pigment paste particles formed on the surface layer of the printed PET-TiO<sub>2</sub>-S<sub>L</sub>-4 fabric, and it has a rough surface and big particles on it. Figure 12e shows some particles of the pigment paste observed on the printed PET-TiO<sub>2</sub>-S<sub>H</sub> surface, while the printed PET-TiO<sub>2</sub>-S<sub>H</sub>-4 fabric is rough with larger pigment paste particles on the surface fabric, as shown in Fig. 12f.

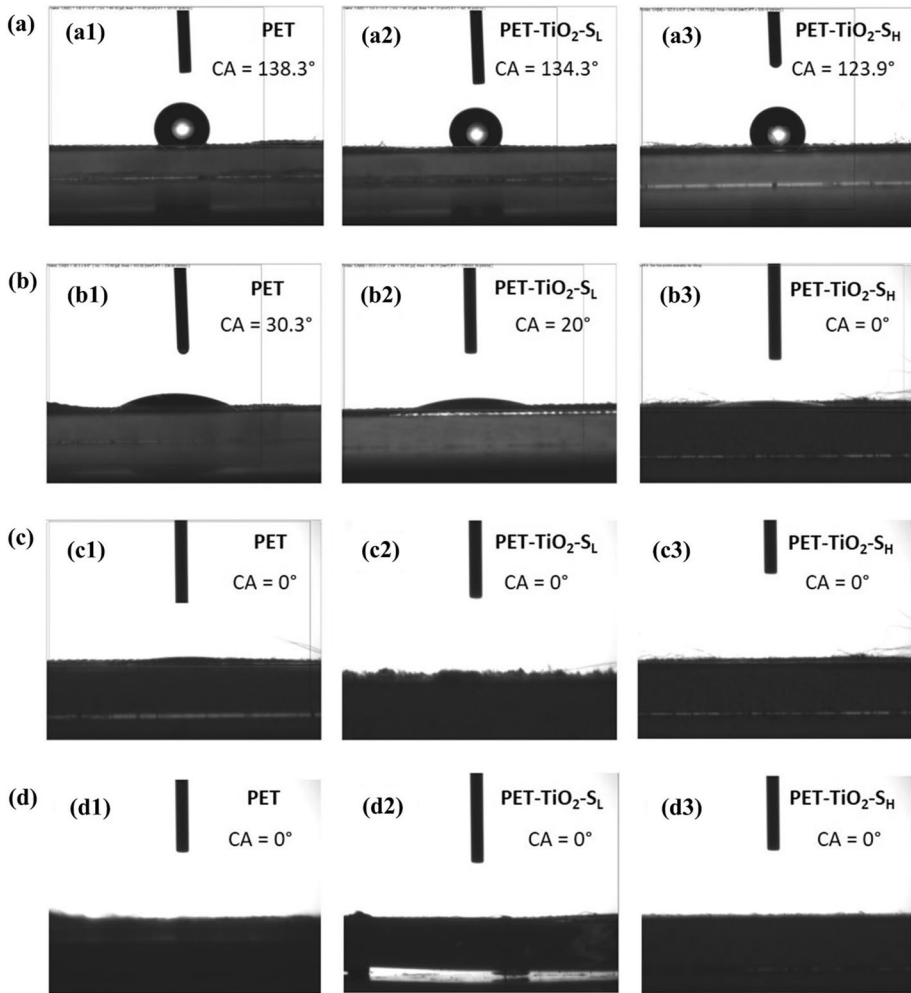


**Fig. 9** Water contact angles of untreated samples (a) and treated samples (b) 1 min, (c) 4 min, and (d) 7 min of PET, PET-TiO<sub>2</sub>-S<sub>L</sub>, and PET-TiO<sub>2</sub>-S<sub>H</sub> samples, respectively

EDS spectroscopy was used to detect the surface chemical elements of the samples, and Fig. 13 shows the weight percentage and relative surface atomic percentages of carbon (C), nitrogen (N), oxygen (O), and copper (Cu) on the outer surface of the samples as the major elements. This is due to the combination of two carbon-containing materials, and the printed samples had substantially greater carbon element content. Cu and N elements are visible in the spectra of the printed fabrics, as they are part of the pigment paste's chemical characteristics. N and Cu elements were found on the surface of the fabric samples, indicating that the printing process is successful. The concentration of the Cu element appeared to be much higher on the PET-TiO<sub>2</sub>-S<sub>L</sub>-4 sample, with a weight ratio of 3.54% and an atomic ratio of 0.73% (Fig. 13d), whereas it is lower in the other printing samples. The higher weight ratio and atomic ratio of Cu indicates that the K/S values were increased on the outer surface of the PET-TiO<sub>2</sub>-S<sub>L</sub>-4 sample. Hence,

**Fig. 10** Photograph of a PET-TiO<sub>2</sub>-S<sub>L</sub> fabric sample with one-time multiple color printing through different plasma etching time, respectively



**Fig. 11** Photographs of printed fabric samples at 7 min of (a) PET, (b) PET-TiO<sub>2</sub>-S<sub>L</sub>, and (c) PET-TiO<sub>2</sub>-S<sub>H</sub> samples, respectively

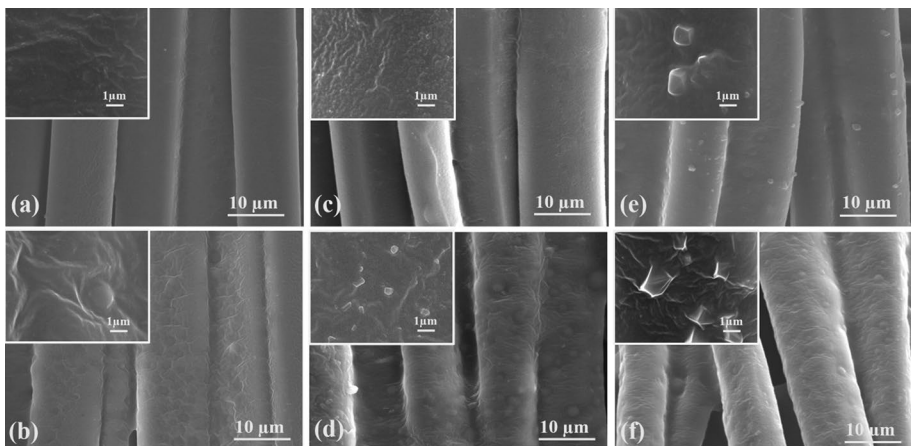


**Fig. 12** The FE-SEM test of printed fabric samples on PET, PET-TiO<sub>2</sub>-S<sub>L</sub>, and PET-TiO<sub>2</sub>-S<sub>H</sub> samples before (a, c, and e) and after (b, d, and f) 4 min plasma etching, respectively

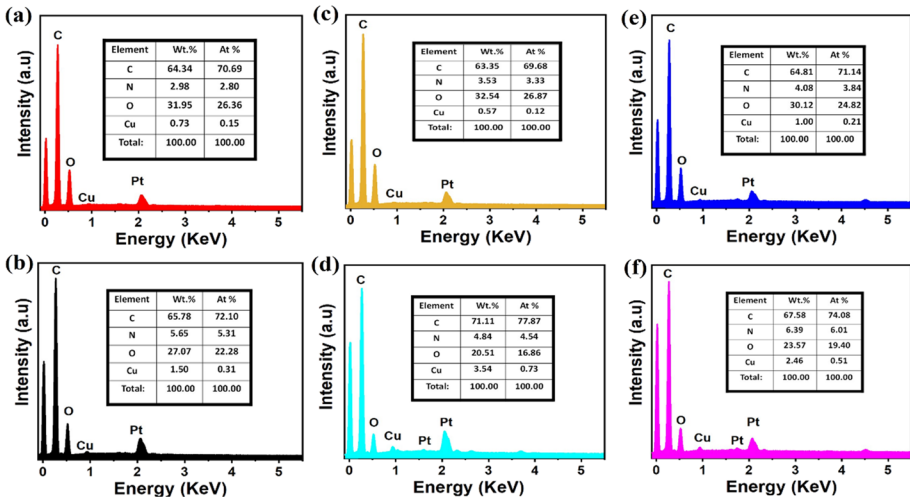


Fig. 13 The EDS test of printed fabric samples on PET, PET-TiO<sub>2</sub>-S<sub>L</sub>, and PET-TiO<sub>2</sub>-S<sub>H</sub> samples before (a, c, and e) and after (b, d, and f) 4 min plasma etching, respectively

the FE-SEM and EDS results reveals the presence of a coating (pigment paste particles) on the surface of the printing samples, although the Ti element is mostly not detected.

The higher K/S result demonstrated a better color strength. The paste printing was carried out in 1 h after plasma treatments. Figure 14 indicates that Ar/O<sub>2</sub> plasma influences the printing properties of fabrics.

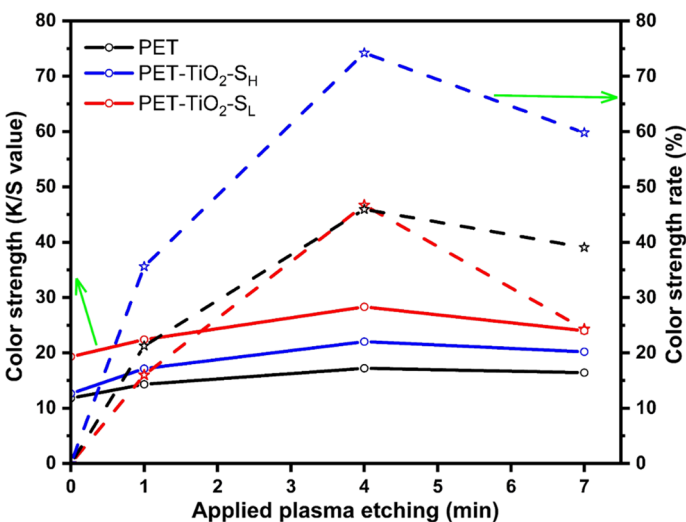


Fig. 14 K/S value and color strength percentage of samples

The K/S values of all samples are increased by plasma treating for 1 and 4 min. However, 7 min plasma treating caused the K/S values decreasing for sample PET-TiO<sub>2</sub>-S<sub>L</sub> and PET-TiO<sub>2</sub>-S<sub>H</sub>. The color strength rate shows similar changes.

The surface roughness also played an important role for K/S value in the print process for its better absorbability to the pigment which size are among 0.5–2.5 μm. On the other hand, with increasing of treating time, more TiO<sub>2</sub> particles were exposed to the surface, it caused the light scattering and diffused surface reflection change which decreased the K/S values [38]. In summary, the higher concentration of TiO<sub>2</sub> reduces the K/S value of the PET fabrics. Therefore, this also explains the lower K/S values of PET-TiO<sub>2</sub>-S<sub>H</sub> samples with different plasma treating times than the PET-TiO<sub>2</sub>-S<sub>L</sub> samples in Fig. 14.

### Fastness Properties: Color Strength (K/S Value)

Table 3 presents the rubbing and washing fastness of the samples using standard measurement methods. Color fastness washing was evaluated for changes in color and staining on the multifiber fabric. The rubbing fastness of the samples was tested in both dry and wet conditions. Pure PET printed fabric shows a fair (3) rating for changing color, while the printed samples at 1, 4, and 7 min, respectively exhibits a fair to good washing fastness rating, ranging from (3–4) to (4), as listed in Table 3. In addition, the change in staining of neighboring fabrics (wool, acrylic, polyester, nylon, cotton, and acetate) is nearly the same for both untreated and treated printed PET fabrics. Correspondingly, the untreated PET-TiO<sub>2</sub>-S<sub>L</sub> and untreated PET-TiO<sub>2</sub>-S<sub>H</sub> printed fabrics are rated as fairly good (3–4), while the samples printed at 1, 4, and 7 min shows a better rating of (4) for washing fastness.

Furthermore, all untreated and treated printed delustered PET fabrics exhibits better washing fastness before and after plasma etching treatment, with no change in staining

**Table 3** Color fastness properties of the printed samples with different plasma treatment times

Samples name	Fastness properties								
	Washing fastness						Alt	Rubbing fastness	
	Staining							Dry	Wet
	Wool	Acrylic	Polyester	Nylon	Cotton	Acetate			
PET-pure	4–5	4–5	4–5	4–5	4–5	5	3	2–3	2–3
PET-1	5	4–5	4–5	4–5	4	5	3–4	4	3–4
PET-4	4–5	5	4–5	4–5	4–5	5	3–4	3	3
PET-7	5	5	4–5	4–5	5	5	4	3	2–3
PET-TiO <sub>2</sub> -S <sub>L</sub>	5	5	5	5	4–5	5	3–4	3–4	3
PET-TiO <sub>2</sub> -S <sub>L</sub> -1	5	5	5	5	5	5	4	4–5	4–5
PET-TiO <sub>2</sub> -S <sub>L</sub> -4	5	5	5	5	5	5	4	4	3–4
PET-TiO <sub>2</sub> -S <sub>L</sub> -7	5	5	5	5	5	5	4	3–4	3
PET-TiO <sub>2</sub> -S <sub>H</sub>	5	5	5	5	4–5	5	3–4	3–4	3
PET-TiO <sub>2</sub> -S <sub>H</sub> -1	5	5	5	5	5	5	4	4–5	4
PET-TiO <sub>2</sub> -S <sub>H</sub> -4	5	5	5	5	5	5	4	3–4	3–4
PET-TiO <sub>2</sub> -S <sub>H</sub> -7	5	5	5	5	5	5	4	3–4	3



of adjacent fabrics (wool, acrylic, polyester, nylon, cotton, and acetate). The dry rubbing fastness of all untreated and treated printing delustered PET fabrics ranged from (3–4) to (4–5), which is slightly better than the untreated and treated printing pure PET fabrics, ranging from (2–3) to (4). Similarly, the wet rubbing fastness of untreated and treated printing pure PET fabrics ranged from (2–3) to (3–4), which is noticeably lower than that of untreated and treated printing delustered PET fabrics that ranged from (3–4) to (4–5). These results indicate that paste printing had a positive impact on improving the fastness properties of treated printing delustered PET samples [39, 40].

## Washing Durability of Samples

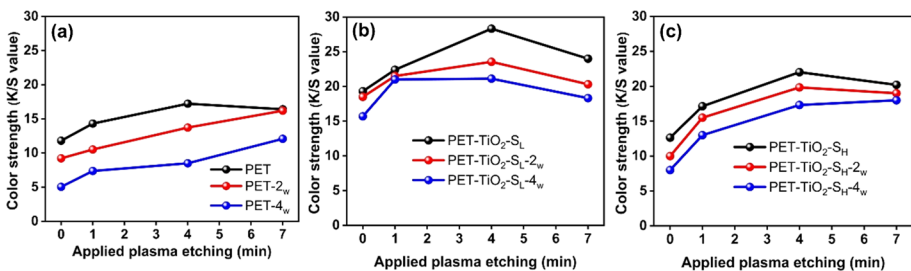
The durability of printed samples was assessed by subjecting them to four washing cycles. Figure 15 demonstrates that both untreated and treated printing samples exhibited a decrease in K/S values following the washing cycles. However, the untreated and treated printing samples on delustered PET fabrics demonstrate superior performance compared to those on pure PET fabrics after 2 and 4 washing cycles.

Figure 15a demonstrates a decrease in paste printing on the surfaces of treated pure PET print samples after undergoing 4 washing cycles. This suggests a lack of interaction between the paste printing and the surfaces of both untreated and treated pure PET fabrics.

The results are shown in Fig. 15b, c suggests that the color strength (K/S) of treated delustered PET prints remained strong even after 4 washing cycles. The pigment paste is still tightly loaded and bonded onto the printed fabric surfaces in this manner. The amount of  $\text{TiO}_2$  particles on the surface has impact on color qualities, including dispersibility and high durability [41]. This might be attributed to the plasma etching treatment of delustered PET fabrics that enhanced the durability toward washing in the presence of  $\text{TiO}_2$  and interaction with the pigment paste.

## The Mechanism Proposed for Plasma Etching Treatment and Fabric Surface Printability

As shown in Fig. 16, a sequential interaction protocol is proposed to elucidate the surface reaction mechanism of plasma selective etching system and screen printing process on  $\text{PET-TiO}_2\text{-S}_L$  fabric surface. Initially, due to the disparate etch rate between  $\text{TiO}_2$  particles and PET fiber in  $\text{O}_2/\text{Ar}$  plasma, a rough surface was generated, providing greater surface area for paste printing molecules absorption. The ion bombardment in the plasma



**Fig. 15** Washing durability K/S values for printed PET-pure samples (a), printed  $\text{PET-TiO}_2\text{-S}_L$  samples (b), and printed  $\text{PET-TiO}_2\text{-S}_H$  samples (c) after 2 and 4 washing cycles

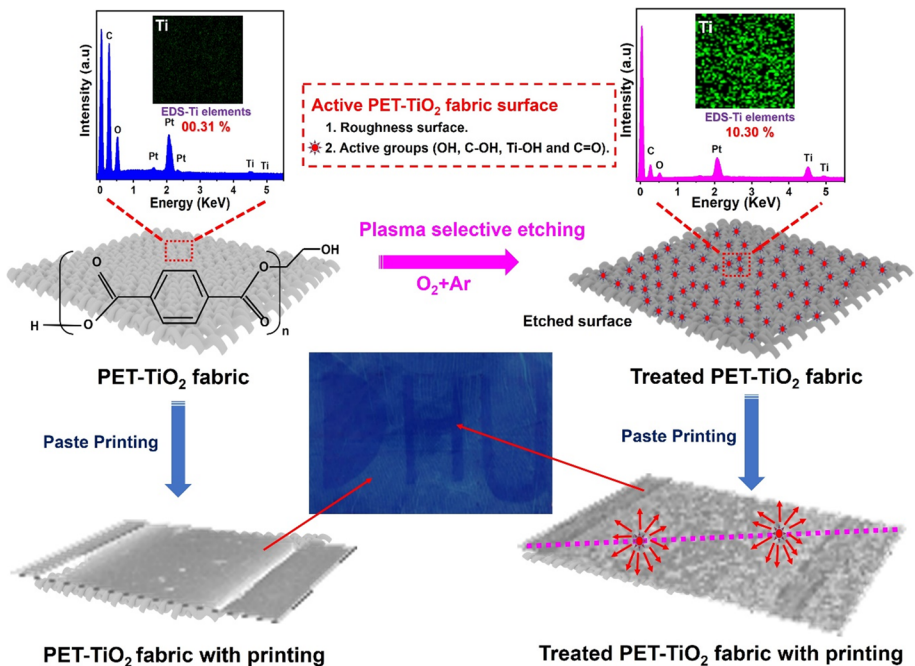


**Fig. 16** The proposed reaction mechanism of pigment paste printing with plasma exposing PET-TiO<sub>2</sub> fabric

breaks the chemical bonds on the fiber surface and strip off surface molecules, which is an efficient mechanism for surface etching of fibers [33, 42, 43]. Additionally, the C1s X-ray photoelectron spectroscopy (XPS) analysis reveals a substantial reduction in C–H content and a corresponding increase in –COOH, –C=O, or C–OH groups on the fiber surface. These changes contribute to the enhanced hydrophilicity of the surface [34]. The result indicates that some of the C–C bonds in polymer surface are broken by the plasma treatments. Then the carbon radicals, formed by the abstraction of hydrogen atoms from the polymer chains, might combine with the oxygen atoms generated in plasma resulting in the formation of the oxygen-containing polar groups on the fabric surface [44]. The high-energy electrons and photons generated in the plasma are considered to play a crucial role in this process [45]. Furthermore, the O1s XPS analysis indicates an increase in Ti–OH groups due to plasma treatment, which also contributes to the enhanced surface hydrophilicity. In summary, the plasma etching treatment creates a rough surface with pores, fissures, and hydrophilic groups, facilitating the absorption of paste printing molecules and improving the printability of the PET-TiO<sub>2</sub> fabric. As a result, the K/S values of the fabric are significantly increased.

## Conclusion

This research work employed the O<sub>2</sub>/Ar plasma etching process operating at 13.56 MHz to enhance the printability of PET fabrics for paste printing. The FE-SEM and AFM results indicate that PET-TiO<sub>2</sub> samples exhibit higher roughness compared to pure PET, which

is attributed to the differential etch rate between TiO<sub>2</sub> particles and the PET fiber. XPS analysis reveals an increase in the oxygen content on the fiber surface for both PET-pure and PET-TiO<sub>2</sub> fabrics, resulting from the introduction of polar groups such as –COOH, –C=O, C–OH, and Ti–OH. Various surface, physical, and chemical properties could be achieved by varying the plasma treatment time to obtain multiple colors and luster in a single printing process. Furthermore, the plasma-treated and printed PET-TiO<sub>2</sub> matrix fabrics exhibits the improved washing and rubbing fastness compared to the untreated samples, highlighting the potential of these techniques for eco-friendly and effective printing production. Overall, this research work findings demonstrated a novel approach for achieving multiple colors and luster with a one-time printing process.

**Acknowledgements** The National Natural Science Foundation of China (Nos. 12075054, 12205040, and 11875104) and the Fundamental Research Funds of Central Universities (Nos. 2232021G-10, 2232019A3-12).

## References

1. Abou Elmaaty T et al (2022) Novel antiviral and antibacterial durable polyester fabrics printed with selenium nanoparticles (SeNPs). *Polymers* 14(5):955
2. Izdebska-Podsiadly J (2019) Application of plasma in printed surfaces and print quality. *Non-thermal plasma technology for polymeric materials*. Elsevier, pp 159–191
3. Agarwal R, Jassal M, Agrawal AK (2021) Durable functionalization of polyethylene terephthalate fabrics using metal oxides nanoparticles. *Colloids Surf, A* 615:126223
4. Owad TT et al (2022) Durable and recoverable hydrophilicity of polyethylene terephthalate fabric prepared with plasma selective etching. *Surf Interfaces* 32:102081
5. Sliman H, Dong X, Zhao T (2020) Functionalization of polyethylene terephthalate knitted fabric with cowpea protein and biopolymer complex: applications for enhancing wettability and UV-Protection properties. *J Colloid Interface Sci* 565:360–367
6. Ibrahim N et al (2013) Enhancing disperse printing and ultraviolet protecting of polyester-containing fabrics via pretreatment with chitosan/polyethylene glycol/dimethylol dihydroxyethylene urea. *J Ind Text* 42(3):269–282
7. Lee H-R, Kim D-J, Lee K-H (2001) Anti-reflective coating for the deep coloring of PET fabrics using an atmospheric pressure plasma technique. *Surf Coat Technol* 142:468–473
8. Zhang F-X, Liang H, Zhang G-X (2016) Colorant-free coloration and superhydrophilic modification of poly (ethylene terephthalate) fabric surface by H<sub>2</sub>O<sub>2</sub> and nano-TiO<sub>2</sub> ultraviolet photocatalysis. *Text Res J* 86(10):1009–1022
9. Chang S et al (2017) Probing polarity of flame retardants and correlating with interaction between flame retardants and PET fiber. *J Colloid Interface Sci* 498:343–350
10. Jamaliniya S, Samei N, Shahidi S (2019) Using low temperature plasma for surface modification of polyester fabric: dyeing and printing improvement. *J Text Inst* 110(5):647–651
11. Salem T et al (2017) Plasma-assisted surface modification of polyester fabric for developing halochromic properties. *Fibers Polym* 18(4):731–740
12. Mehravani B et al (2022) In situ synthesis of copper nanoparticles on dielectric barrier discharge plasma-treated polyester fabrics at different reaction pHs. *ACS Appl Polym Mater* 4(5):3908–3918
13. Hossain MA et al (2020) The effect of O<sub>2</sub> plasma treatment and PA 6 coating on digital ink-jet printing of PET non-woven fabric. *J Text Inst* 111(8):1184–1190
14. Abou Elmaaty T et al (2018) One step thermochromic pigment printing and Ag NPs antibacterial functional finishing of cotton and cotton/PET fabrics. *Fibers Polym* 19(11):2317–2323
15. Edward NW, Goswami P (2018) Plasma-based treatments of textiles for water repellency. *Waterproof and water repellent textiles and clothing*. Elsevier, pp 215–232
16. Agnhage T, Perwuelz A, Behary N (2016) Eco-innovative coloration and surface modification of woven polyester fabric using bio-based materials and plasma technology. *Ind Crops Prod* 86:334–341
17. Pransilp P et al (2016) Surface modification of cotton fabrics by gas plasmas for color strength and adhesion by inkjet ink printing. *Appl Surf Sci* 364:208–220
18. Cheng F et al (2019) The effect of atmospheric pressure glow discharge plasma treatment on the dyeing properties of silk fabric. *Plasma Sci Technol* 22(1):015503
19. Islam MT, Asaduzzaman S (2019) Environmentally-friendly textile finishing. In: Shabbir M (ed) *Textiles and clothing*. Wiley, pp 101–129. <https://doi.org/10.1002/9781119526599>

20. Pransilp P et al (2012) Plasma nano-modification of poly (ethylene terephthalate) fabric for pigment adhesion enhancement. *J Nanosci Nanotechnol* 12(1):481–488
21. Rashid MM et al (2022) Sono-synthesis of cellulose-TiO<sub>2</sub> nanocomposite adsorbent for fast cleaning of anionic dyes containing wastewater. *J Water Process Eng* 47:102799
22. Liu K et al (2023) Hydroxyethyl methyl cellulose controls the diffusion behavior of pico-liter scale ink droplets on silk to improve inkjet printing performance. *Int J Biol Macromol* 224:1252–1265
23. Zhang C et al (2019) Study on the physical-morphological and chemical properties of silk fabric surface modified with multiple ambient gas plasma for inkjet printing. *Appl Surf Sci* 490:157–164
24. Zille A (2020) Plasma technology in fashion and textiles. *Sustainable technologies for fashion and textiles*. Elsevier, pp 117–142
25. Lakshmanan SO, Raghavendran G (2017) Low water-consumption technologies for textile production. *Sustainable fibres and textiles*. Elsevier, pp 243–265
26. Xu Y et al (2022) Enhanced reactive dye inkjet printing performance of antimicrobial silk fabrics surface modified with plasma and chitosan. *Fibers Polym* 23(9):2586–2596
27. Hassan A et al (2019) Plasma-etching and modification of polyethylene for improved surface structure, wettability and optical behavior. *Surf Rev Lett* 26(07):1850220
28. Singh M, Vajpayee M, Ledwani L (2020) Eco-friendly surface modification and nanofinishing of textile polymers to enhance functionalisation. In: Ledwani L, Sangwai J (eds) *Nanotechnology for energy and environmental engineering*. Springer, Cham, pp 529–559. [https://doi.org/10.1007/978-3-030-33774-2\\_23](https://doi.org/10.1007/978-3-030-33774-2_23)
29. Tungtriratanakul S et al. (2015) Effect of nano TiO<sub>2</sub> treatment on disperse dyeing and self-cleaning properties of PET fabric. In: *Applied mechanics and materials*. Trans Tech Publ
30. Baggerman J, Visser R, Collart E (1994) Ion-induced etching of organic polymers in argon and oxygen radio-frequency plasmas. *J Appl Phys* 75(2):758–769
31. Kylián O et al (2009) Removal of model proteins using beams of argon ions, oxygen atoms and molecules: mimicking the action of low-pressure Ar/O<sub>2</sub> ICP discharges. *Plasma Process Polym* 6(4):255–261
32. Bourceanu G, Gheorghiu MD, Moisa C (1985) Effect of the gas nature and etching time of poly(ethylene terephthalate) (PET) film on the high-frequency plasma. *Rev Roum Phys* 30:145–150
33. Amberg M et al (2022) Surface modification of recycled polymers in comparison to virgin polymers using Ar/O<sub>2</sub> plasma etching. *Plasma Process Polym* 19(12):e2200068
34. Elabid AE et al (2016) Improving the low temperature dyeability of polyethylene terephthalate fabric with dispersive dyes by atmospheric pressure plasma discharge. *Appl Surf Sci* 375:26–34
35. Radoičić MB et al (2015) Influence of TiO<sub>2</sub> nanoparticles on formation mechanism of PANI/TiO<sub>2</sub> nanocomposite coating on PET fabric and its structural and electrical properties. *Surf Coat Technol* 278:38–47
36. Siddig EAA et al (2022) Antibacterial through plasma-exposed titanium nanoparticles on delustered PET/TiO<sub>2</sub> fabric surfaces. *Mater Lett* 308:131189
37. Meng F et al (2020) Mechanism study on TiO<sub>2</sub> inducing O<sub>2</sub><sup>-</sup> and OH radicals in O<sub>3</sub>/H<sub>2</sub>O<sub>2</sub> system for high-efficiency NO oxidation. *J Hazard Mater* 399:123033
38. Cho DH (2004) Experimental study on dyeing technical PET yarns having different TiO<sub>2</sub> contents. *Fibers Polym* 5(4):321–326
39. Jafari H, Khajeh Mehrizi M, Fattahi S (2016) The effect of inorganic nanoparticles on camouflage properties of cotton/polyester fabrics. *Progr Color, Colorants Coat* 9(1):29–40
40. Al-Etaibi AM, El-Asasery MA (2020) Nano TiO<sub>2</sub> imparting multifunctional performance on dyed polyester fabrics with some disperse dyes using high temperature dyeing as an environmentally benign method. *Int J Environ Res Public Health* 17(4):1377
41. Noman MT et al (2018) A novel green stabilization of TiO<sub>2</sub> nanoparticles onto cotton. *Fibers Polym* 19(11):2268–2277
42. Dmitriev S et al (2000) A high-frequency plasma-discharge effect on poly (ethylene) terephthalate films exposed to heavy ions. *Nucl Instrum Methods Phys Res, Sect B* 171(4):448–454
43. Savoji H et al (2015) Plasma-etching for controlled modification of structural and mechanical properties of electrospun PET scaffolds. *Plasma Process Polym* 12(4):314–327
44. Wang C et al (2008) Influence of atmospheric pressure plasma treatment time on penetration depth of surface modification into fabric. *Appl Surf Sci* 254(8):2499–2505
45. Amel EE et al (2016) Synergistic Effect of atmospheric pressure plasma pre-treatment on alkaline etching of polyethylene terephthalate fabrics and Films. *Plasma Sci Technol* 18(4):346

Springer Nature or its licensor (e.g. a society or other partner) holds exclusive rights to this article under a publishing agreement with the author(s) or other rightsholder(s); author self-archiving of the accepted manuscript version of this article is solely governed by the terms of such publishing agreement and applicable law.

## Authors and Affiliations

**Tarig T. A. Owad<sup>1</sup> · Amel E. A. Elabid<sup>2</sup> · Renad E. M. Salih<sup>1</sup> · Syed Rashedul Islam<sup>3</sup> · Bilal Zaarour<sup>4</sup> · Yu Zhang<sup>1</sup> · Yu Xu<sup>1,5,7</sup> · Jie Min<sup>6</sup> · Jing Zhang<sup>1,5,7</sup>**

✉ Yu Xu  
yuxu@dhu.edu.cn

✉ Jing Zhang  
jingzh@dhu.edu.cn

<sup>1</sup> New Energy Materials and Devices, College of Science, Donghua University, Shanghai 201620, China

<sup>2</sup> Faculty of Industries Engineering and Technology, University of Gezira, Wad Medani 21111, Sudan

<sup>3</sup> Engineering Research Center of Technical Textiles, Ministry of Education, College of Textiles, Donghua University, Shanghai 201620, China

<sup>4</sup> Textile Industries Mechanical Engineering and Techniques Department, Faculty of Mechanical and Electrical Engineering, Damascus University, Damascus, Syria

<sup>5</sup> Magnetic Confinement Fusion Research Center, Ministry of Education of the People's Republic of China, Shanghai 201620, China

<sup>6</sup> College of Chemistry and Chemical Engineering and Biotechnology, Key Laboratory of Textile Science and Technology, Ministry of Education, Donghua University, Shanghai 201620, China

<sup>7</sup> Textile Key Laboratory for Advanced Plasma Technology and Application, China National Textile & Apparel Council, Shanghai 201620, China